GEOMETRIES, ELECTRONIC STRUCTURES AND ELECTRONIC ABSORPTION SPECTRA OF SILICON DICHLORIDE SUBSTITUTED PHTHALOCYANINE FOR DYE SENSITIZED SOLAR CELLS

P. M. Anbarasan[*], P. Senthil kumar, M. Geetha, R. Govindan, S. Manimegalai and K. Velmurugan

Department of Physics, Periyar University, Salem – 636 011, Tamilnadu, India

Abstract

The geometries, electronic structures, polarizabilities, and hyperpolarizabilities of Silicon dichloride substituted phthalocyanine dye sensitizer were studied based on Density Functional Theory (DFT) using the hybrid functional B3LYP. Ultraviolet-Visible (UV-Vis) spectrum was investigated by using a hybrid method which combines the single-excitation configuration interactions (CIS) with DFT, i.e. CIS-DFT(B3LYP). Features of the electronic absorption spectrum in the visible and near-UV regions were assigned based on CIS-DFT calculations. The absorption bands are assigned to n→π* transitions. Calculated results suggest that the three lowest energy excited states of Silicon dichloride substituted phthalocyanine are due to photoinduced electron transfer processes. The interfacial electron transfer between semiconductor TiO_2 electrode and dye sensitizer is due to an electron injection process from excited dye to the semiconductor's conduction band. The role of Silicon dichloride in phthalocyanine geometries, electronic structures and electronic absorption spectra were analysed and these results were concluded that Silicon dichloride substituted phthalocyanine used in Dye Sensitized Solar Cells (DSSC) give a good conversion efficiency.

Introduction

The new technologies for direct solar energy conversion have gained more attention in the last few years. In particular, Dye Sensitized Solar Cells (DSSCs) are promising in terms of efficiency and low cost [1-3]. Upon light excitation, the adsorbed dye molecules inject electrons from their excited states into the conduction band of the semiconductor. The electrons are brought back to the oxidized dye through an external circuit, a platinum counter electrode, and a redox system (typically I^-/I_3^-). The use of a nanostructured TiO_2 film together with the Ru(dcbpy)2(NCS)2[dcbpy=4,4'-dicarboxy-2,2'-bipyridine] (RuN3 for short) dye introduced by Gratzel and co-workers [1,2] was a breakthrough in terms of a commercial application. An overall conversion efficiency of ~10% has been achieved. Since then, extensive attention has been paid to this research field [4-10].

To date, ruthenium (II) polypyridyl complexes have proved to be the best sensitizers for dye-sensitized nanostructured TiO_2 solar cells [1,2]. However, the main drawback of those sensitizers is the lack of absorption in the far-red/near-IR region of the solar spectrum [11]. To further improve the performance of these devices, it is imperative to enhance their response in the abovementioned wavelength region. Phthalocyanines possess intensive absorption in the far-red/near-IR region; are known for their excellent chemical, light, and thermal stability; and have the appropriate redox properties for sensitization of large band-gap semiconductors, e.g., TiO_2 [12] making them attractive for DSSC. However, there are some problems to be solved for phthalocyanines to be used in solar cell applications. The typical phthalocyanines explored for sensitization of large band-gap semiconductors are free-base or metallic ones, substituted by carboxylic or sulfonic acid groups for attachment to the semiconductor surface [13-17]. They are poorly soluble in organic solvents, for example, ethanol and chloroform, which makes it difficult to synthesize, separate, and purify these kinds of phthalocyanines. Another major problem with phthalocyanines is their strong tendency to aggregate on the semiconductor surface, which to some extent results in very low IPCE (typically < 4%) of solar cells [13-17] Gratzel and co-workers [18] reported a strikingly high IPCE of 45% in the near-infrared region

[*] Corresponding Author, *Email*: anbarasanpm@gmail.com, Tel: +91-0427-2345766, 2345520, Fax: +91-0427-2345565, 2345124

for a sandwich solar cell based on a zinc tetracarboxyl phthalocyanine (ZnTcPc)-sensitized nanostructured TiO_2 electrode when surface aggregation of the sensitizer was avoided. In this study investigating the geometry, Natural Bonding Analysis (NBO), Nonlinear Optical properties (NLO), Electronic absorption spectrum analysis of Silicon dichloride substituted phthalocyanine for dye sensitized solar cells using Quantum chemical calculations.

Phthalocyanines (Pc) are strong absorption in the visible region (the Q band; $\lambda_{max} \approx 700$ nm), are highly versatile and stable chromophores with unique photophysical and photochemical properties that make them, alone or in combination with many other electro and photoactive moieties, ideal building blocks for the construction of molecular materials with special electronic and optical properties [19]. Among the Pc derivatives, the axially substituted silicon phthalocyanines (SiPc) are of great interest because the axial substitutions make it possible to prevent unwanted aggregation in solution [19].

Computational Methods

The computations of the geometries, electronic structures, polarizabilities and hyperpolarizabilities for dye Silicon dichloride substituted phthalocyanine were done using DFT with Gaussian 03 package [20]. The DFT was treated according to hybrid functionals Becke's three parameter and the Lee-Yang-Parr (B3LYP) [21–23], and all calculations were performed without any symmetry constraints by using polarized triple-zeta 6-311++G(d,p) basis sets. The Natural Bonding Orbital (NBO) analysis was performed using restricted Hartree-Fock (RHF) with 6-311++G(d,p) basis set. The electronic absorption spectrum requires calculation of the allowed excitations and oscillator strengths. These calculations were done using a hybrid method which combines the single-excitation configuration interactions (CIS) with Density Functional Theory (DFT), i.e. CIS-DFT(B3LYP) with the 6-311++G(d,p) basis set in vacuum and acetonitrile

solution, and the non-equilibrium version of the polarizable continuum model (PCM) [24,25] was adopted for calculating the solvent effects.

Results and Discussion
The geometric structure

The Silicon dichloride substituted phthalocyanine was optimized using B3LYP/6-311++G(d,p). The optimized geometry of the Silicon dichloride substituted phthalocyanine is shown in Figure 1, and the bond lengths, bond angles and dihedral angles are listed in Table 1. The crystal structure of the exact title compound is compared with XRD [26] values and we can find that most of the optimized bond lengths, bond angles and dihedral angles.

Figure 1. Optimized geometry structure of the Silicon dichloride substituted phthalocyanine
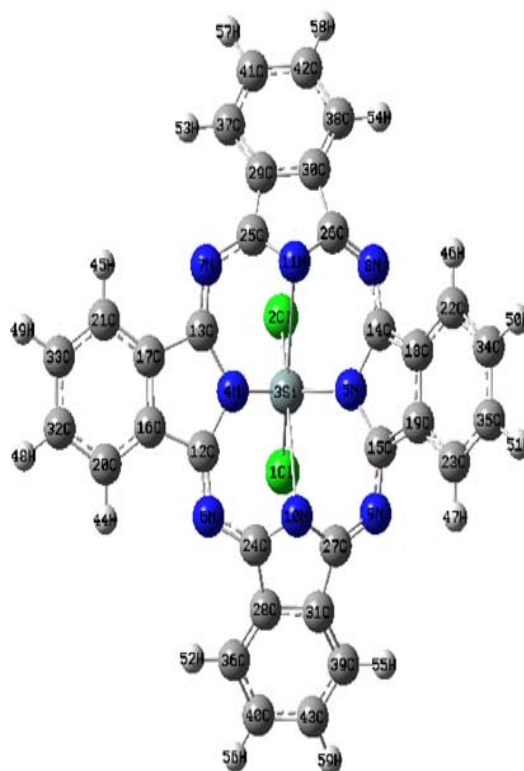
Table 1. Selected Bond lengths (in Å) and bond angles (in degree) of the dye Silicon dichloride substituted phthalocyanines.

Parameters	B3LYP/6-311++G(d,p)	XRD [26]
Bond Length		
Si3-Cl1	2.1608	-
Si3-N4	1.8354	1.92
N4-C12	1.4385	1.375
N6-C12	1.3191	1.321
C12-C16	1.4975	1.449
C16-C17	1.4180	1.386
C16-C20	1.3808	1.391
C20-C32	1.4063	1.380
C32-C33	1.3918	1.386
Bond Angles		
N4-C12-N6	132.40	127.9
C12-N6-C13	105.73	107.2
C12-N6-C24	120.09	121.5
N6-C12-C16	108.35	109.8
N6-C12-C16	118.84	122.3
C12-C16-C17	106.99	106.6
C12-C16-C20	131.74	131.9
C17-C16-C20	121.25	121.6
C16-C20-C32	117.49	116.7
C20-C32-C33	121.24	121.5

Electronic structures and charges

NBO analysis was performed in order to analyze the charge populations of the dye Silicon dichloride substituted phthalocyanine. The frontier molecular orbitals (MO) energies and corresponding density of state of the dye Silicon dichloride substituted phthalocyanine is shown in Figure 2. The HOMO–LUMO gap of the dye Silicon dichloride substituted phthalocyanine in vacuum is 1.89 eV.

Figure 2: The frontier molecular orbital energies and corresponding density of state (DOS) spectrum of Silicon dichloride substituted phthalocyanines dye.
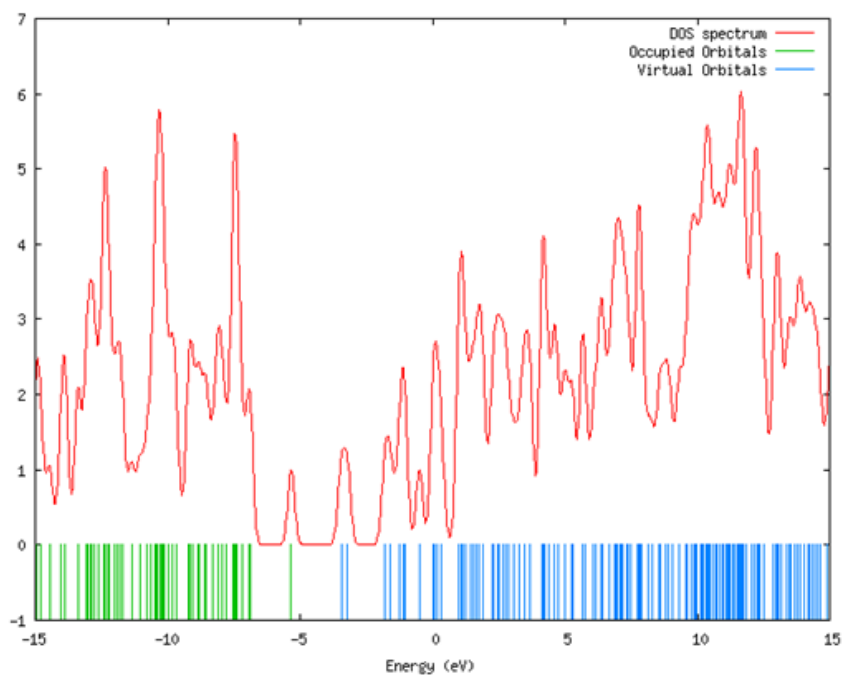
While the calculated HOMO and LUMO energies of the bare $Ti_{38}O_{76}$ cluster as a model for nanocrystalline are -6.55 and -2.77 eV, respectively, resulting in a HOMO–LUMO gap of 3.78 eV, the lowest transition is reduced to 3.20 eV according to TD-DFT, and this value is slightly smaller than typical band gap of TiO_2 nanoparticles with nm size [27]. Furthermore, the HOMO, LUMO and HOMO–LUMO gap of $(TiO_2)_{60}$ cluster is   -7.52, -2.97 and 4.55 eV (B3LYP/VDZ), respectively [28]. Taking into account of the cluster size effects and the calculated HOMO, LUMO, HOMO–LUMO gap of the dye Silicon dichloride substituted phthalocyanine, $Ti_{38}O_{76}$ and $(TiO_2)_{60}$ clusters, we can find that the HOMO energies of these dyes fall within the TiO_2 gap.

The above data also reveal the interfacial electron transfer between semiconductor TiO_2 electrode and the dye sensitizer Silicon dichloride substituted phthalocyanine is electron injection processes from excited dye to the semiconductor conduction band. This is a kind of typical interfacial electron transfer reaction [29].

Polarizability and hyperpolarizability

Polarizabilities and hyperpolarizabilities characterize the response of a system in an applied electric field [30]. They determine not only the strength of molecular interactions (long-range intermolecular induction, dispersion forces, etc.) as well as the cross sections of different scattering and collision processes, but also the nonlinear optical properties (NLO) of the system [31, 32]. It has been found that the dye sensitizer hemicyanine system, which has high NLO property, usually possesses high photoelectric conversion performance [33]. In order to investigate the relationships among photocurrent generation, molecular structures and NLO, the polarizabilities and hyperpolarizabilities of Silicon dichloride substituted phthalocyanine was calculated. Here, the polarizability and the first hyperpolarizabilities are computed using B3LYP/6-311++G(d,p) method. The definitions [31,32] for the isotropic polarizability is

$$\alpha = \frac{1}{3}\left(\alpha_{XX} + \alpha_{YY} + \alpha_{ZZ}\right)$$
(1)

The polarizability anisotropy invariant is

$$\Delta\alpha = \left[\frac{\left(\alpha_{XX} - \alpha_{YY}\right)^2 + \left(\alpha_{YY} - \alpha_{ZZ}\right)^2 + \left(\alpha_{ZZ} - \alpha_{XX}\right)^2}{2}\right]^{\frac{1}{2}}$$
(2)

and the average hyperpolarizability is

$$\beta_{\square} = \frac{1}{5}\sum_i\left(\beta_{iiZ} + \beta_{iZi} + \beta_{Zii}\right)$$
(3)

Where, α_{XX}, α_{YY}, and α_{ZZ} are tensor components of polarizability; β_{iiZ}, β_{iZi}, and β_{Zii} (i from X to Z) are tensor components of hyperpolarizability.

Tables 2 and 3 list the values of the polarizabilities and hyperpolarizabilities of the dye Silicon dichloride substituted phthalocyanine. In addition to the individual tensor components of the polarizabilties and the first hyperpolarizabilities, the isotropic polarizability, polarizability anisotropy invariant and hyperpolarizability are also calculated. The calculated isotropic polarizability of Silicon dichloride substituted phthalocyanine is 239.03 a.u. However, the calculated isotropic polarizability of JK16, JK17, dye 1, dye 2, D5, DST and DSS is 759.9, 1015.5, 694.7, 785.7, 510.6, 611.2 and 802.9 a.u., respectively [33, 34]. The above data indicate that the donor-conjugate π bridge-acceptor (D-π-A) chain-like dyes have stronger response for external electric field. Whereas, for dye sensitizers D5, DST, DSS, JK16, JK17, dye 1 and dye 2, on the basis of the published photo-to-current conversion efficiencies, the similarity and the difference of geometries, and the calculated isotropic polarizabilities, it is found that the longer the length of the conjugate bridge in similar dyes, the larger the polarizability of the dye molecule, and the lower the photo-to-current conversion efficiency. This may be due to the fact that the longer conjugate π bridge enlarged the delocalization of electrons, thus it enhanced the response of the external field, but the enlarged delocalization may be not favorable to generate charge separated state effectively. So it induces the lower photo-to-current conversion efficiency.

Table 2: Polarizability (α) of the dye Silicon dichloride substituted phthalocyanine (in a.u.)

α_{xx}	α_{xy}	α_{yy}	α_{xz}	α_{yz}	α_{zz}	α	$\Delta\alpha$
-221.35	0.0002	-214.25	-0.0149	-1.4619	-281.51	239.03	64.006

Table 3: Hyperpolarizability (β) of the dye Silicon dichloride substituted phthalocyanine (in a.u.).

β_{xxx}	β_{xxy}	β_{xyy}	β_{yyy}	β_{xxz}	β_{xyz}	β_{yyz}	β_{xzz}	β_{yzz}	β_{zzz}	β_{ii}
0.073	-1.792	0.0311	-38.40	-94.71	-0.013	51.72	-0.055	-3.456	-3.207	27.71

Electronic absorption spectra and sensitized mechanism

The UV-Vis spectra of Silicon dichloride substituted phthalocyanine were measured [26] in acetonitrile solution, and it is found that the absorption bands centered at 702 nm in UV region. Electronic absorption spectra of Silicon dichloride substituted phthlocyanine in vacuum and solvent were performed using CIS-DFT(B3LYP)/6-311++G(d,p) calculations, and the results are shown in Fig. 3. It is observed that, for Silicon dichloride substituted phthalocyanine, the absorption in the visible region is much weaker than that in the UV region. The results of CIS-DFT have an appreciable red-shift in vacuum and solvent, and the degree of red-shift in solvent is more significant than that in vacuum. The discrepancy between experimental and solvent effects in CIS-DFT calculations may result from two aspects. The first aspect is smaller gap of materials which induces smaller excited energies. The other is solvent effects. Experimental measurements of electronic absorptions are usually performed in solution. Solvent, especially polar solvent, could affect the geometry and electronic structure as well as the properties of molecules through the long-range interaction between solute molecule and solvent molecule. For these reasons it is more difficult to make the CIS-DFT calculation is consistent with quantitatively. Though the discrepancy exists, the CIS-DFT calculations are capable of describing the spectral features of Silicon dichloride substituted phthalocyanine because of the agreement of line shape and relative strength as compared with the experimental and calculated values.

Figure 3: UV/Vis electronic absorption spectra of Silicon dichloride substituted phthalocyanine
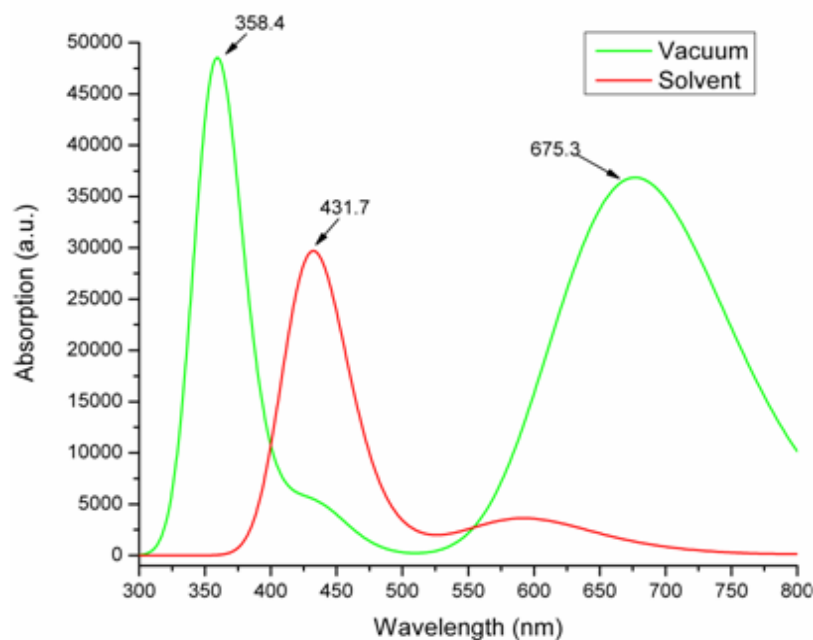
The HOMO-LUMO gap of Silicon dichloride substituted phthalocyanine in acetonitrile at CIS-DFT/6-311++G(d,p) theory level is smaller than that in vacuum. This fact indicates that the solvent effects stabilize the frontier orbitals of Silicon dichloride substituted phthalocyanine. So it induces the smaller intensities and red-shift of the absorption as compared with that in vacuum.

In order to obtain the microscopic information about the electronic transitions, the corresponding MO properties are checked. The absorption in visible and near-UV region is the most important region for photo-to-current conversion, so only the 20 lowest singlet/singlet transitions of the absorption band in visible and near-UV region for Silicon dichloride substituted phthalocyanine is listed in Table 4. The data of Table 4 and Figure 6 are based on the CIS-DFT/6-311++G(d,p) results with solvent effects involved.

Figure 4: Isodensity plot (isodensity contour = 0.02 a.u.) of the frontier orbitals of Silicon dichloride substituted phthalocyanines and corresponding orbital energies (in eV).
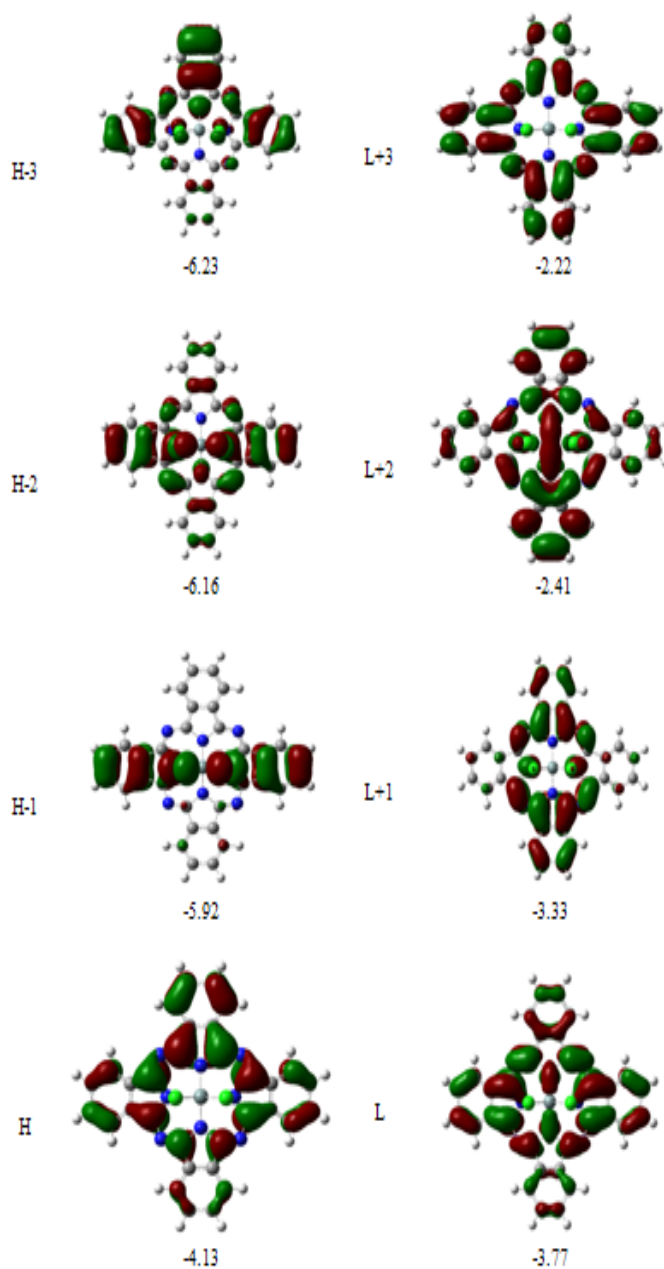
Table 4. Computed excitation energies, electronic transition configurations and oscillator strengths (f) for the optical transitions with f > 0.01 of the absorption bands in visible and near- UV region for the dye Silicon dichloride substituted phthalocyanine in acetonitrile solvent

State	Configurations composition (corresponding transition orbitals)	Excitation energy (eV/nm)	Oscillator strength (f)
1	0.49584 (156 →157)	0.7412 / 1672.84	0.0759
2	0.60993 (156 →158)	1.0577 / 1172.16	0.1139
4	0.60464 (156 →160) 0.27407 (156 →161) -0.12284 (156 →162)	2.0986 / 590.79	0.0446
10	0.22273 (151 →157) 0.50359 (153 →157) -0.14785 (156 →160) 0.19611 (156 →161) -0.27219 (156 →162)	2.6166 / 473.84	0.0258
13	-0.22820 (148 →157) -0.13398 (150 →157) -0.13786 (151 →158) 0.43412 (152 →157) 0.14327 (153 →158) -0.14332 (154 →157) -0.37749 (155 →158)	2.7835 / 445.43	0.0408
16	0.12559 (148 →157) 0.58101 (150 →157) 0.21283 (152 →157) -0.18458 (153 →158) -0.13969 (156 →165)	2.8772 / 430.93	0.1167
17	-0.12406 (147 →157) 0.39788 (149 →157) 0.49808 (151 →157) 0.51005 (148 →157)	2.8850 / 429.76	0.2212
18	-0.10677 (151 →158) 0.10496 (152 →157) 0.42771 (153 →158)	2.9128 / 425.66	0.0170

This indicates that the transitions are photoinduced charge transfer processes, thus the excitations generate charge separated states, which should favour the electron injection from the excited dye to semiconductor surface.

The solar energy to electricity conversion efficiency (η) under AM 1.5 white-light irradiation can be obtained from the following formula:

$$\eta(\%) = \frac{J_{SC}[mAcm^{-2}]V_{OC}[V]ff}{I_0[mWcm^{-2}]} \times 100$$

Where I_0 is the photon flux, J_{sc} is the short-circuit photocurrent density, and V_{oc} is the open-circuit photovoltage, and ff represents the fill factor [35]. At present, the J_{sc}, the V_{oc}, and the ff are only obtained by experiment, the relationship among these quantities and the electronic structure of dye is still unknown. The analytical relationship between V_{oc} and E_{LUMO} may exist. According to the sensitized mechanism (electron injected from the excited dyes to the semiconductor conduction band) and single electron and single state approximation, there is an energy relationship:

$$eV_{oc} = E_{LUMO}-E_{CB}$$

Where, E_{CB} is the energy of the semiconductor's conduction band edge. So the Voc may be obtained applying the following formula:

$$V_{oc} = \frac{(E_{LUMO}-E_{CB})}{e}$$

It induces that the higher the E_{LUMO}, the larger the V_{oc}. The results of organic dye sensitizer JK16 and JK17 [34], D-ST and D-SS also proved the tendency [36] (JK16: LUMO = -2.73 eV, V_{oc} = 0.74 V; JK17: LUMO = -2.87 eV, V_{oc} = 0.67 V; D-SS: LUMO = -2.91 eV, V_{oc} = 0.70 V; D-ST: LUMO = -2.83 eV, V_{oc} = 0.73 V). Certainly, this formula expects further test by experiment and theoretical calculation. The J_{sc} is determined by two processes, one is the rate of electron injection from the excited dyes to the conduction band of semiconductor, and the other is the rate of redox between the excited dyes and electrolyte. Electrolyte effect on the redox processes is very complex, and it is not taken into account in the present calculations. This indicates that most of excited states of Silicon dichloride substituted phthalocyanine have larger absorption coefficient, and then with shorter lifetime for the excited states, so it results in the higher electron injection rate which leads to the larger J_{sc} of

Silicon dichloride substituted phthalocyanine. On the basis of above analysis, it is clear that the Silicon dichloride substituted phthalocyanine has better performance in DSSC.

Conclusions

The geometries, electronic structures, polarizabilities, and hyperpolarizabilities of Silicon dichloride substituted phthalocyanine dye was studied by density functional theory with hybrid functional B3LYP, and the UV-Vis spectra were investigated by using CIS methods. The NBO results suggest that Silicon dichloride substituted phthalocyanine is a (D-π-A) system. The calculated isotropic polarizability of Silicon dichloride substituted phthalocyanine is 239.03 a.u. The calculated polarizability anisotropy invariant of Silicon dichloride substituted phthalocyanine is 64.006 a.u. The hyperpolarizability of Silicon dichloride substituted phthalocyanine is 27.71 (in a.u). The electronic absorption spectral features in visible and near-UV region were assigned based on the qualitative agreement to CIS-DFT calculations. The absorptions are all ascribed to n→π* transition. The three excited states with the lowest excited energies of Silicon dichloride substituted phthalocyanine are photoinduced electron transfer processes that contribute sensitization of photo-to-current conversion processes. The interfacial electron transfer between semiconductor TiO_2 electrode and dye sensitizer Silicon dichloride substituted phthalocyanine is electron injection process from excited dye as donor to the semiconductor conduction band. Based on the analysis of geometries, electronic structures, and electronics absorption spectrum properties of Silicon dichloride substituted phthalocyanine, the role of Silicon dichloride in phthalocyanine is as follows: it enlarged the distance between electron donor group and semiconductor surface, and decreased the timescale of the electron injection rate, resulted in giving lower conversion efficiency. This indicates that the choice of the appropriate conjugate bridge in dye sensitizer is very important to improve the performance of DSSC.

Acknowledgement

References

1. B. O'Regan, M. Gratzel, Nature 353 (1991) 737-739.
2. M. K. Nazeeruddin, A. Kay, I. Rodicio, R. Humphry-Baker, E. Muller, P. Liska, N. Vlachopoulos, M. Gratzel, J. Am. Chem. Soc. 115 (1993) 6382.
3. Hagfeldt, M. Gratzel, Chem. Rev. 95 (1995) 49.
4. Hagfeldt, M. Gratzel, Acc. Chem. Res. 33 (2000) 269.
5. A. Kelly, G. Meyer, J. Coord. Chem. Rev. 211 (2001) 295.
6. P. Bonhote, J.E. Moser, R. Humphry-Baker, N. Vlachopoulos, M. Zakeeruddin, L. Walder, M. Gratzel, J. Am. Chem. Soc. 121 (1999) 1324.
7. K. Kalyanasundaram, M. Gratzel, Coord. Chem. Rev. 77 (1998) 347.
8. S. Y. Huang, G. Schlichthorl, A. J. Nozik, M. Gratzel, A. J. Frank, J. Phys. Chem. B 101 (1997) 2576.
9. K. Hara, K. Sayama, Y. Ohga, A. Shinpo, S. Suga, H. Arakawa, Chem. Commun. (2001) 569.
10. K. Schwarzburg, F. Willig, J. Phys. Chem. B 103 (1999) 5743.
11. M. K. Nazeeruddin, P. Pechy, T. Renouard, S. M. Zakeeruddin, R. Humphry-Baker, P. Comte, P. Liska, L. Cevey, E. Costa, V. Shklover, L. Spiccia, G. B. Deacon, C. A. Bignozzi, M. Gratzel, J. Am. Chem. Soc. 123 (2001) 1613.
12. C. Leznoff, A.B. P. Lever, Phthalocyanines: Properties and applications, VCH: New York (1993) Vol. 1, (1993) Vol. 2, (1993) Vol. 3, (1996) Vol. 4.
13. J. Fang, L. Su, J. Wu, Y. Shen, Z. Lu, New J. Chem. 21 (1997) 1303.
14. Y. Shen, L. Wang, Z. Lu, Y. Wei, Q. Zhou, H. Mao, H. Xu, Thin Solid Films 257 (1995) 144.
15. J. Fang, J. Wu, X. Lu, Y. Shen, Z. Lu, Chem. Phys. Lett. 270 (1997) 145.
16. H. Yanagi, S. Chen, P. A. Lee, K. W. Nebesny, N. R. Armstrong, A. Fujishima, J. Phys. Chem. 100 (1996) 5447.
17. H. Deng, Z. Lu, H. Mao, H. Xu, Chem. Phys. 221 (1997) 323.
18. M. K. Nazeeruddin, R. Humphry-Baker, M. Gratzel, D. Wohrle, G. Schnurpfeil, G. Schneider, A. Hirth, N. Trombach, J. Porphyrins Phthalocyanines 3 (1999) 230.
19. N. B. McKeown, Phthalocyanine Materials: Synthesis, Structure and Function, Cambridge University Press, Cambridge (1998).
20. M.J. Frisch, G.W. Trucks, H.B. Schlegel, G.E. Scuseria, M.A. Robb, J.R. Cheeseman, J.A. Montgomery Jr., T. Vreven, K.N. Kudin, J.C. Burant, J.M. Millam, S.S. Iyengar, J. Tomasi, V. Barone, B. Mennucci, M. Cossi, G. Scalmani, N. Rega, G.A. Petersson, H. Nakatsuji, M. Hada, M. Ehara, K. Toyota, R. Fukuda, J. Hasegawa, M. Ishida, T. Nakajima, Y. Honda, O. Kitao, H. Nakai, M. Klene, X. Li, J.E. Knox, H.P. Hratchian, J.B.

Cross, C. Adamo, J. Jaramillo, R. Gomperts, R.E. Stratmann, O. Yazyev, A.J. Austin, R. Cammi, C. Pomelli, J.W. Ochterski, P.Y. Ayala, K. Morokuma, G.A. Voth, P. Salvador, J.J. Dannenberg, V.G. Zakrzewski, S.Dapprich, A.D. Daniels, M.C. Strain, O. Farkas, D.K. Malick, A.D. Rabuck, K. Raghavachari, J.B. Foresman, J.V. Ortiz, Q. Cui, A.G. Baboul, S. Clifford, J.Cioslowski, B.B. Stefanov, G. Liu, A. Liashenko, P. Piskorz, I. Komaromi, R.L. Martin, D.J. Fox, T. Keith, M.A. Al-Laham, C.Y. Peng, A. Nanayakkara, M. Challacombe, P.M.W. Gill, B. Johnson, W. Chen, M.W. Wong, C. Gonzalez, J.A. Pople, Gaussian 03, Gaussian, Inc., Pittsburgh, PA (2003).

21. A.D. Becke, J. Chem. Phys. 98 (1993) 5648-5652.
22. B. Miehlich, A. Savin, H. Stoll, H. Preuss, Chem. Phys. Lett. 157 (1989) 200-206.
23. Lee, W. Yang, R.G. Parr, Phys. Rev. B. 37 (1988) 785-789.
24. V. Barone, M. Cossi, J. Phys. Chem. A, 102 (1998) 1995-2001.
25. M. Cossi, N. Rega, G. Scalmani, V. Barone, J. Comput. Chem. 24 (2003) 669-681.
26. Braun, B. C. Titeca, A. Ceulemans, J. Porphyrins Phthalocyanines 5 (2001) 33–43

27. M.K. Nazeeruddin, F. De Angelis, S. Fantacci, A. Selloni, G. Viscardi, P. Liska, S.Ito, B. Takeru, M. Gratzel, J. Am. Chem. Soc. 127 (2005) 16835-16847.
28. M.J. Lundqvist, M. Nilsing, P. Persson, S. Lunell, Int. J. Quantum Chem. 106 (2006) 3214-3234.
29. D.F. Waston, G.J. Meyer, Annu. Rev. Phys. Chem. 56 (2005) 119-156.
30. C. R. Zhang, H. S. Chen, and G. H. Wang, Chem. Res. Chin. U. 20 (2004) 640-646.
31. Y. Sun, X. Chen, L. Sun, X. Guo, W. Lu, Chem.Phys. Lett. 381 (2003) 397-403.
32. O. Christiansen, J. Gauss, J. F. Stanton, Chem.Phys. Lett. 305 (1999) 147-155.
33. Z. S. Wang, Y. Y. Huang, C. H. Huang, J. Zheng, H.M. Cheng, S. J. Tian, Synth. Met. 14 (2000) 201-207.
34. C.R. Zhang, Y.Z. Wu, Y.H. Chen, H.S. Chen, Acta Phys. Chim. Sin. 25 (2009) 53-60.
35. K. Hara, T. Sato, R. Katoh, A. Furube, Y. Ohga, A. Shinpo, S. Suga, K. Sayama, H.Sugihara, H. Arakawa, J. Phys. Chem. B. 107 (2003) 597-606.
36. C.R. Zhang, Z.J. Liu, Y.H. Chen, H.S. Chen, Y.Z. Wu, L.H. Yuan, J. Mol. Struct. 899 (2009) 86-93.